a spherical shell of ~7.5-km depth below Europa's surface and a conductivity of 2.75 S m^{-1} for Earth's oceans (*20*) would be 90% that of a highly conducting sphere with a phase lag relative to the primary field of 25°. The amplitudes of the induced magnetic moment for E4, E14, and E26 would be reduced by the phase lag (*21*). If the ocean were thicker, but still close to the surface, or if the conductivity were higher, the phase lag would decrease, and the amplitude of the response would increase.

On passes E4, E12, E14, E19, and E26, currents induced by the time-varying primary field in a Europan ionosphere may contribute to the magnetic perturbation. Elsewhere (*18*), we have calculated the signature of induced currents flowing above the surface, close to Galileo's trajectory, in a conducting shell of larger than 1 R_E radius. Based on the measured ionospheric density and scale height (*22*) and measured (*23*) or modeled (*24*) atmospheric properties, we find that ionospheric currents fail to account for the observations by an order of magnitude.

The case for a subsurface electrical conductor on a planetary-wide scale passed the test of the E26 flyby with flying colors. Although the electrically conducting layer need not be salty water, water is the most probable medium on Europa. Geological evidence has been interpreted as consistent with surface effects of subsurface liquid water, but the defining features could have been formed in the distant past. The magnetometer result makes it likely that liquid water persists in the present epoch.

References and Notes

1. R. Greeley *et al.*, *Icarus* **135**, 25 (1998).
2. R. T. Pappalardo, J. W. Head, R. Greeley, *Sci. Am.* **281**, 54 (1999).
3. G. V. Hoppa, B. R. Tufts, R. Greenberg, P. E. Geissler, *Science* **285**, 1899 (1999).
4. R. Greenberg *et al.*, *Icarus* **141**, 263 (1999).
5. M. G. Kivelson *et al.*, *Science* **276**, 1239 (1997).
6. K. K. Khurana *et al.*, *Nature* **395**, 777 (1998).
7. M. G. Kivelson *et al.*, *J. Geophys. Res.* **104**, 4609 (1999).
8. D. S. Colburn and R. T. Reynolds, *Icarus* **63**, 39 (1985).
9. F. M. Neubauer, *J. Geophys. Res.*, **103**, 19843 (1998).
10. The coordinate system used in this paper (referred to as Ephio) is Europa-centric with x along the corotating plasma flow, y radially in toward Jupiter, and z parallel to Jupiter's spin axis. In conventional units of A m^2, the magnetic moment is $4\pi R_E^3 M/\mu_o$, where μ_o is the magnetic permeability.
11. Our rationale for ignoring passes at altitude greater than 2000 km is that at 2000-km altitude and directly over the induced magnetic pole, the signal from an internal magnetic moment of ~100 nT (see E11, Table 1) is less than 8.4 nT. Away from the pole, the signal amplitude becomes even smaller. Such small amplitude signals are difficult to interpret given the levels of fluctuations typical of the plasma background.
12. The components of the magnetospheric field are plotted with a broad line to take into account variations of the primary field that occur at other than the synodic period. Such variations are expected because Europa's radial distance and latitude vary from pass to pass as a result of the ellipticity and slight inclination of Europa's orbit and because of temporal variations in the plasma sheet.
13. The measured magnetic moment is obtained by fitting the difference between the measured field components and the smoothly varying background field to a dipole field over the intervals tabulated in Table 1. The components of the dipole moment are obtained by a least squares technique.
14. F. M. Neubauer, *J. Geophys. Res.* **85**, 1171 (1980).
15. D. J. Southwood, M. G. Kivelson, R. J. Walker, J. A. Slavin, *J. Geophys. Res.* **85**, 5959 (1980).
16. Web figures 1 and 2 are available at Science *Online* at www.sciencemag.org/feature/data/1052679.shl.
17. F. M. Neubauer, *J. Geophys. Res.* **104**, 28671 (1999).
18. C. Zimmer, K. K. Khurana, M. G. Kivelson, *Icarus*, in press. This work used the electromagnetic induction solution for multiple concentric shells given in (*19*).
19. W. D. Parkinson, *Introduction to Geomagnetism* (Elsevier, New York, 1983), p. 313.
20. R. B. Montgomery, in *American Institute of Physics Handbook*, D. E. Gray, Ed. (McGraw-Hill, New York, 1963), pp. 125–127.
21. This can be understood by noting that in the inset to Fig. 3, the primary field was increasing in the hour before each of those encounters. Thus, a phase lag of 25° or 0.6 hours implies that the induced currents are responding to a smaller primary field.
22. A. J. Kliore, D. P Hinson, F. M. Flasar, A. F. Nagy, T. E. Cravens, *Science* **277**, 355 (1997).
23. D. T. Hall, P. D. Feldman, M. A. McGrath, D. F. Strobel, *Astrophys. J.* **499**, 475 (1998).
24. J. Saur, D. F. Strobel, F. M. Neubauer, *J. Geophys. Res.* **103**, 19947 (1998).

25. We are grateful to our programmers, S. Joy and J. Mafi, for their devoted efforts to acquire and process the data on a short time scale and during holiday periods. Support for this work was provided in part by contract JPL 958694 from NASA's Jet Propulsion Laboratory (JPL), which manages the Galileo mission. Special thanks are due to D. Bindschadler, C. Polanskey, J. Erickson, and others at JPL who worked to design a Europa pass optimized to provide the test that we report here.

31 May 2000; accepted 10 July 2000

Molecular Analysis of Plant Migration and Refugia in the Arctic

Richard J. Abbott,[1]* Lisa C. Smith,[1] Richard I. Milne,[1] Robert M. M. Crawford,[1] Kirsten Wolff,[1,2] Jean Balfour[1]

The arctic flora is thought to have originated during the late Tertiary, approximately 3 million years ago. Plant migration routes during colonization of the Arctic are currently unknown, and uncertainty remains over where arctic plants survived Pleistocene glaciations. A phylogenetic analysis of chloroplast DNA variation in the purple saxifrage (*Saxifraga oppositifolia*) indicates that this plant first occurred in the Arctic in western Beringia before it migrated east and west to achieve a circumpolar distribution. The geographical distribution of chloroplast DNA variation in the species supports the hypothesis that, during Pleistocene glaciations, some plant refugia were located in the Arctic as well as at more southern latitudes.

Throughout much of the Tertiary, the Arctic supported continuous forests (*1, 2*). Only toward the end of this period does fossil evidence show that certain present-day arctic plants were established and widely distributed in the Arctic, although extensive areas of lowland tundra were absent (*3, 4*). Many arctic plants are thought to have originated in the high mountain ranges of central Asia and North America (*1, 5, 6*), to have spread northward to the Arctic as global temperatures fell in the late Tertiary, and to have achieved a circumpolar distribution by the late Tertiary to early Pleistocene (*5*). However, phytogeographic and fossil evidence to support these proposals is either lacking or fragmentary. Consequently, the migration routes followed by plants during the early colonization of the Arctic remain unknown.

During the Pleistocene, the distribution and ranges of arctic plants were greatly affected by the advance and retreat of ice sheets, and it was initially supposed that their survival depended on migration southward, ahead of advancing ice sheets (*7*). However, since the discovery that large parts of the Arctic and Subarctic in northwest America and eastern Siberia (i.e., Beringia) were never glaciated (*5, 8, 9*), these northern areas are also thought to have served as important refugia for arctic plants during Pleistocene glaciations (*5*).

We surveyed chloroplast DNA (cpDNA) variation throughout a large part of the distribution of the circumpolar arctic-alpine plant, *Saxifraga oppositifolia* (purple saxifrage). This is a long-lived, perennial, herbaceous, and outcrossing plant (*10*) that is distributed throughout the Arctic and in mountain ranges to the south (*11*). Both diploid and

[1]Division of Environmental and Evolutionary Biology, Harold Mitchell Building, School of Biology, University of St. Andrews, St. Andrews, Fife KY16 9TH, UK. [2]Department of Agricultural and Environmental Sciences, Ridley Building, University of Newcastle, Newcastle-upon-Tyne NE1 7RU, UK.

*To whom correspondence should be addressed. E-mail: rja@st-and.ac.uk

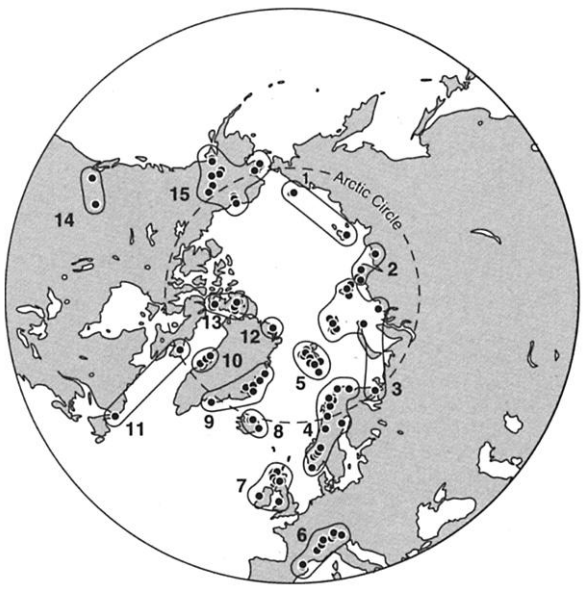

Fig. 1. Locations of populations of *S. oppositifolia* sampled from 15 regions. 1, east Siberia; 2, Taymyr; 3, northwest Russia; 4, Scandinavia; 5, Svalbard; 6, Alps and Pyrenees; 7, British Isles; 8, Iceland; 9, east Greenland; 10, west Greenland; 11, east Canada; 12, north Greenland; 13, the Canadian Arctic; 14, west Canada and the United States; and 15, Alaska.

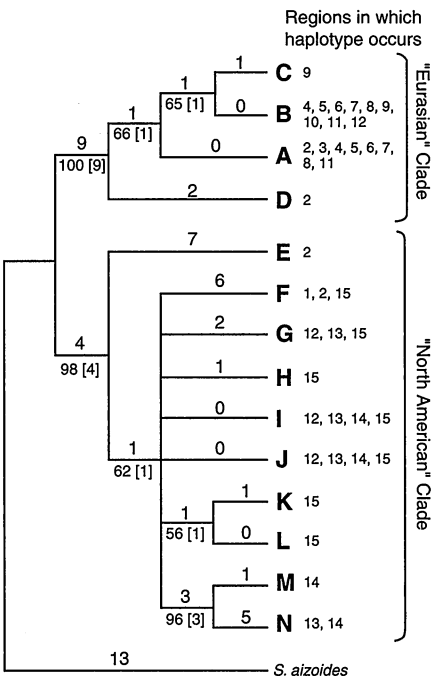

Fig. 2. Strict consensus of 27 most parsimonious trees for cpDNA haplotypes detected in *S. oppositifolia* (A through N) and in one accession of *S. aizoides* used as an outgroup. Numbers above branches are the minimum branch lengths (from all most parsimonious trees). Below the branches are bootstrap support values followed by Bremer decay indices in brackets. Numbers to the right of each haplotype represent the regions (Fig. 1) in which a haplotype was found. When autapomorphies were excluded from analysis, the consistency index, retention index, and homoplasy index equaled 0.923, 0.968, and 0.078, respectively.

tetraploid forms of the species exist, but there is no known taxonomic pattern to this variation (*12*). cpDNA is inherited maternally in the Saxifragaceae (*13*). We examined cpDNA restriction site variation among 548 plants sampled from 90 different populations distributed over 15 designated regions [Fig. 1 and Web table 1 (*14*)]. DNA extracts from leaf material desiccated with silica gel were purified and subjected to restriction site analysis using established procedures (*15*). Southern blots were probed with *Vigna radiata* (mung bean) cpDNA fragments (*16*). The analysis (*17*) resolved 37 restriction site and 11 insertion and deletion (indel) mutations, whose presence or absence in individuals enabled identification of 14 cpDNA haplotypes (A through N) [see Web table 2 (*14*)]. We assessed genealogical relationships among haplotypes based on maximum parsimony and neighbor-joining distance analyses using PAUP, version 4.0b (*18*).

The strict consensus maximum parsimony tree (Fig. 2) shows that *S. oppositifolia* is divided into two clades. The first clade, with 100% bootstrap support, contains four haplotypes (A through D) and is distributed westward from the Taymyr Peninsula in north-central Siberia, through Europe and Greenland, to Newfoundland and Baffin Island on the eastern seaboard of North America. The second clade, with 98% support, contains 10 haplotypes (E through N) and is distributed eastward from the Taymyr Peninsula, through northeast Siberia and northern North America (apart from Newfoundland and Baffin Island), to north Greenland (Peary Land). The topology of the neighbor-joining tree was compatible with that of the strict consensus maximum parsimony tree.

The different geographical distributions of the two clades closely match those of two widely distributed subspecies of *S. oppositifolia*, subsp. *oppositifolia* and subsp. *glandulisepala,* respectively (*11*), which are distinguished mainly by the presence of glandular hairs on sepals in subsp. *glandulisepala* (*19*). The branch lengths of the two cpDNA clades (Fig. 2) suggest that they diverged from their common ancestor early in the evolution of *S. oppositifolia* and have evolved mainly in geographical isolation from that time. Despite this, very little morphological change has evolved between the two lineages. The possibility that one lineage obtained its cpDNA from another species through hybridization cannot be excluded, because rare examples of interspecific hybridization involving *S. oppositifolia* are known or suspected (*12*). However, an entire cpDNA lineage composed of several haplotypes would not be captured unless the hybridization event was ancient and diversification had occurred within the lineage since then.

The two cpDNA lineages remain separate throughout their respective distributions, except in the Taymyr and north Greenland regions (Fig. 2). Haplotypes D and E, which are basal to the mainly Eurasian and mainly North American clades, respectively, co-occur in Taymyr and are found nowhere else. A possible explanation of this distribution pattern is that the species first occurred in the Arctic in western Beringia before migrating in east and west directions to obtain a circumpolar distribution. *S. oppositifolia* is also distributed through the Sino-Himalayan region of central Asia where several other species of *Saxifraga* sect. *Porphyrion* subsect. *Oppositifoliae* occur, which like *S. oppositifolia* have opposite leaves (*12, 20*). It is conceivable, therefore, that *S. oppositifolia* is derived from ancestral stock located in the high mountains of central Asia, which migrated to the Arctic in northern Siberia along mountain ranges that connect these two regions. The discovery of late Tertiary macrofossils of *S. oppositifolia* in the Canadian Arctic Archipelago (*4*) and in north Greenland (*3*) suggests that migration of the species from Beringia eastward to north Greenland would have been completed before the start of the Pleistocene.

We recorded high levels of cpDNA diversity within the three North American regions examined (Alaska, the Canadian Arctic, and west Canada and the western United States) and also in north Greenland and in the region of the Taymyr Peninsula (Table 1). Other regions surveyed contained much less diversity, except east Canada, which exhibited high total diversity but no variation within the two populations sampled. The high level of cpDNA diversity in *S. oppositifolia* in Alaska supports fossil evidence (*21, 22*) that a major refugium for arctic plants was present in eastern Beringia during the last full-glacial period. High diversity is expected in parts of a species' current distribution that were refugia, unless variation has been reduced by genetic drift due to small population size (*23,*

Table 1. Frequencies of cpDNA haplotypes within regions and estimates of average gene diversity within populations (H_S), total gene diversity (H_T), and the proportion of total diversity due to differences between populations (G_{ST}) calculated with HAPLODIV (*30*). N_p and N_i are the number of populations and the number of individuals sampled within regions, respectively. Standard errors in parentheses are not given when less than three populations were sampled per regions, when less than three individuals were surveyed in some populations within a region, or when the errors were not calculated (nc).

Parameter	Regional data														
	East Siberia	Taymyr	North-west Russia	Scand-inavia	Svalbard	Alps and Pyrenees	British Isles	Iceland	East Green-land	West Green-land	East Canada	North Green-land	Canadian Arctic	West Canada/ USA	Alaska
								Number							
N_p	2	4	11	14	9	9	7	3	6	3	2	1	5	2	12
N_i	15	23	40	34	40	67	24	15	45	23	10	38	35	20	119
								Frequency							
Haplotype															
A	0	0.348	1.000	0.176	0.100	0.866	0.792	0.133	0	0	0.600	0	0	0	0
B	0	0	0	0.823	0.900	0.134	0.208	0.867	0.956	1.000	0.400	0.342	0	0	0
C	0	0	0	0	0	0	0	0	0.044	0	0	0	0	0	0
D	0	0.174	0	0	0	0	0	0	0	0	0	0	0	0	0
E	0	0.304	0	0	0	0	0	0	0	0	0	0	0	0	0
F	1.000	0.174	0	0	0	0	0	0	0	0	0	0	0	0	0.286
G	0	0	0	0	0	0	0	0	0	0	0	0.289	0.057	0	0.008
H	0	0	0	0	0	0	0	0	0	0	0	0	0	0	0.017
I	0	0	0	0	0	0	0	0	0	0	0	0.132	0.343	0.250	0.176
J	0	0	0	0	0	0	0	0	0	0	0	0.237	0.543	0.200	0.471
K	0	0	0	0	0	0	0	0	0	0	0	0	0	0	0.008
L	0	0	0	0	0	0	0	0	0	0	0	0	0	0	0.034
M	0	0	0	0	0	0	0	0	0	0	0	0	0	0.500	0
N	0	0	0	0	0	0	0	0	0	0	0	0	0.057	0.050	0
								Average gene diversity estimates							
H_S	0.000	0.266 (0.156)	0.000	0.000	0.079	0.058 (0.041)	0.095 (0.095)	0.200 (0.200)	0.030 (0.030)	0.000	0.000	0.745 (0.028)	0.562 (0.118)	0.322	0.283 (0.064)
H_T	0.000	0.917 (0.026)	0.000	0.363	0.093	0.268 (0.157)	0.381 (0.170)	0.267 (0.196)	0.032 (0.307)	0.000	1.000	–	0.600 (0.082)	1.000	0.629 (0.099)
G_{ST}	0.000	0.710 (0.200)	0.000	1.000	0.151	0.784 (0.202)	0.750 (0.243)	0.250 (nc)	0.050 (nc)	0.000	1.000	–	0.115 (0.117)	0.678	0.550 (0.087)

24). The possibility that this northern refugium extended eastward to unglaciated parts of the Canadian high Arctic (*22*) and to north Greenland is not excluded by our results. All three regions have two high-frequency haplotypes (I and J) in common, and they contain high levels of cpDNA diversity (Table 1). High cpDNA diversity within regions could also result from postglacial colonization by migrants from different refugia having different cpDNA haplotypes. This could explain, in part, the high level of cpDNA diversity found in north Greenland where representatives of the mainly Eurasian lineage (haplotype B) and mainly North American lineage (haplotypes G, I, and J) co-occur. However, there is no indication that the same effect explains the high cpDNA diversity within Alaska or the Canadian high Arctic based on the geographical distributions of haplotypes present in these two regions and the adjacent areas.

High cpDNA diversity found in material sampled from the Taymyr region is of interest because the southeastern part of the Taymyr Peninsula and much of northeast Siberia remained unglaciated during the Pleistocene (*8, 25*). It is feasible, therefore, that representatives of both major cpDNA lineages persisted there during the last full-glacial period. The lack of diversity found in material from northeast Siberia is surprising, but only material from Kotelny and Wrangel islands was analyzed from this region.

Low cpDNA diversity is evident throughout much of the distribution of the mainly Eurasian lineage of purple saxifrage (Table 1), which mostly occupies areas that were heavily glaciated during the Pleistocene (*9*). Haplotype A, which is fixed in material from northwest Russia and is common in the Alps and the British Isles, tends to be replaced by haplotype B in Scandinavia, Svalbard, Iceland, Greenland, and east Baffin Island. This might indicate that haplotypes A and B were distributed in different refugia during the last glaciation (and possibly earlier glaciations) from which migrants colonized deglaciated areas in postglacial times. However, it is not possible to tell from the data where these haplotypes survived the glaciation(s). Fossil evidence shows that arctic-alpine plants occurred in areas to the south, west, and east of the main ice sheets that covered northern Europe and northwest Russia during the last full-glacial period (*26*), as well as to the south and east of the ice sheets in North America (*22, 27*). It is likely that migrants from these areas colonized much of Europe, northwest Russia, Iceland, Greenland, and northeast America during the postglacial period. The present study has shown that a previous estimate of five different cpDNA haplotypes occurring in one population of *S. oppositifolia* in Svalbard (*16*) was incorrect [see Web table 3 (*14*)]. Only two haplotypes (A and B) occur on Svalbard. This result supports the proposal that there is no molecular evidence for the local survival of *S. oppositifolia* within Svalbard or Norway during the last full-glacial period (*28*).

This study shows that an improved knowledge of past migration routes and locations of important Pleistocene refugia for arctic plants can be obtained from surveys of cpDNA variation throughout their present distributions. Further studies of this kind should lead to a more complete understanding of arctic plant evolution since the late Tertiary and make clear whether isolation in glacial refugia was as important in shaping patterns of biodiversity within arctic plants as in temperate species (*29*).

References and Notes

1. D. F. Murray, in *Arctic and Alpine Biodiversity: Patterns, Causes and Ecosystem Consequences*, F. S. Chapin and C. Körner, Eds. (Springer, Heidelberg, Germany, 1995), pp. 21–32.
2. E. E. McIver and J. F. Basinger, *Ann. Mo. Bot. Gard.* **86**, 523 (1999).
3. O. Bennike and J. Böcher, *Arctic* **43**, 331 (1990).

4. J. V. Matthews and L. E. Ovenden, *Arctic* **43**, 324 (1990).
5. E. Hultén, *Outline of the History of Arctic and Boreal Biota During the Quaternary Period* (Cramer, New York, 1937).
6. K. O. Hedberg, *Bot. J. Linn. Soc.* **109**, 377 (1992).
7. D. F. Murray, in *Evolution Today: Proceedings of the Second International Congress of Systematic and Evolutionary Biology*, G. E. Scudder and J. L. Reveal, Eds. (Hunt Institute for Botanical Documentation, Carnegie Mellon University, Pittsburgh, PA, 1981), pp. 11–20.
8. D. M. Hopkins, Ed., *The Bering Land Bridge* (Stanford Univ. Press, Stanford, CA, 1967).
9. B. Frenzel, *Science* **161**, 637 (1968).
10. M. Stenström and U. Molau, *Arct. Alp. Res.* **24**, 337 (1992).
11. E. Hultén and M. Fries, *Atlas of North European Vascular Plants* (Koeltz Scientific, Königstein, Germany, 1986).
12. D. A. Webb and R. J. Gornall, *Saxifrages of Europe: With Notes on African, American and Some Asiatic Species* (Helm, London, 1989).
13. D. E. Soltis, P. E. Soltis, B. D. Ness, *J. Hered.* **81**, 168 (1990).
14. Supplemental Web material is available at www.sciencemag.org/feature/data/1050967.shl.
15. R. I. Milne, R. J. Abbott, K. Wolff, D. F. Chamberlain, *Am. J. Bot.* **86**, 1776 (1999).
16. R. J. Abbott, H. M. Chapman, R. M. M. Crawford, D. G. Forbes, *Mol. Ecol.* **4**, 199 (1995).
17. All samples were surveyed for restriction site variation using four enzyme:probe combinations (Bcl 1 × MB3, MB7; Eco R1 × MB3, MB7) (MB, mung bean), which, in a preliminary analysis, resolved considerable cpDNA variation in the species. These combinations distinguished all cpDNA haplotypes detected in the study, except K from L. Several individuals of each haplotype, sampled from throughout the geographical distribution of a haplotype, were further examined to determine the number of restriction site and indel differences among haplotypes over an additional 45 enzyme:probe combinations (Alu 1 × MB3, 7, 12; Bam H1 × MB3, 7; Bcl 1 × MB5+6; Bgl 2 × MB3, 7, 12; Cfo 1 × MB3, 5+6, 12; Cla 1 × MB3, 5+6, 7; Dra 1 × MB2, 3, 5+6, 7, 12; Eco R1 × MB5+6, 12; Hae 3 × MB2, 3, 5+6, 7, 12; Hinf 1 × MB3, 5+6, 7; Hpa 2 × MB1, 2, 3, 5+6, 7, 12; Rsa 1 × 3, 7; Sac 1 × MB3, 5+6, 7; Sal 1 × MB3, 7; and Pvu 2 × MB3, 7). In so doing, haplotype K was distinguished from L by a single site mutation.
18. D. L. Swofford, *PAUP: Phylogenetic Analysis Using Parsimony, Version 4.0b* (Sinauer, Sunderland, MA, 1998). Maximum parsimony trees were obtained with Wagner parsimony and involved a heuristic search with tree bisection-reconnection branch swapping, STEEPEST DESCENT off, MULTREES on, and ACCTRAN on. The robustness of trees was assessed by bootstrap percentages (after 1000 replications) and Bremer indices.
19. E. Hultén, *Bot. Not.* **126**, 459 (1973).
20. R. J. Gornall, unpublished data.
21. L. C. Cwynar, *Ecol. Monogr.* **52**, 1 (1982).
22. N. O. Tremblay and D. J. Schoen, *Mol. Ecol.* **8**, 1187 (1999).
23. H. P. Comes and J. W. Kadereit, *Trends Plant Sci.* **3**, 432 (1998).
24. G. M. Hewitt, *Biol. J. Linn. Soc.* **68**, 87 (1999).
25. J. I. Svendsen *et al.*, *Boreas* **28**, 234 (1999).
26. H. H. Birks, *Diss. Bot.* **234**, 129 (1994).
27. J. C. Ritchie, *Acta. Bot. Fenn.* **144**, 81 (1992).
28. T. M. Gabrielsen, K. Bachmann, K. S. Jakobsen, C. Brochmann, *Mol. Ecol.* **6**, 831 (1997).
29. K. J. Willis and R. J. Whittaker, *Science* **287**, 1406 (2000).
30. O. Pons and R. J. Petit, *Theor. Appl. Genet.* **90**, 462 (1995).
31. We thank the many colleagues who supplied us with plant material for analysis, especially F. Bretagnolle, C. Brochmann, T. Gabrielsen, U. Malm, and M. Stenström. The work was supported by a grant from the UK Natural Environment Research Council Special Topic Programme in Arctic Terrestrial Ecology (R.J.A and R.M.M.C).

3 April 2000; accepted 11 July 2000

Structure of Yeast Poly(A) Polymerase Alone and in Complex with 3′-dATP

Joel Bard,[1] Alexander M. Zhelkovsky,[2] Steffen Helmling,[2] Thomas N. Earnest,[3] Claire L. Moore,[2] Andrew Bohm[1,4]*

Polyadenylate [poly(A)] polymerase (PAP) catalyzes the addition of a polyadenosine tail to almost all eukaryotic messenger RNAs (mRNAs). The crystal structure of the PAP from *Saccharomyces cerevisiae* (Pap1) has been solved to 2.6 angstroms, both alone and in complex with 3′-deoxyadenosine triphosphate (3′-dATP). Like other nucleic acid polymerases, Pap1 is composed of three domains that encircle the active site. The arrangement of these domains, however, is quite different from that seen in polymerases that use a template to select and position their incoming nucleotides. The first two domains are functionally analogous to polymerase palm and fingers domains. The third domain is attached to the fingers domain and is known to interact with the single-stranded RNA primer. In the nucleotide complex, two molecules of 3′-dATP are bound to Pap1. One occupies the position of the incoming base, prior to its addition to the mRNA chain. The other is believed to occupy the position of the 3′ end of the mRNA primer.

Polyadenylation provides a universal handle by which transport and translation machinery can recognize and physically manipulate mRNAs. In eukaryotic organisms, addition of the poly(A) tail facilitates the transport of mRNA from the nucleus (*1*) and helps regulate mRNA stability (*2*). Interactions between proteins bound to the poly(A) tail and the 5′ end of mRNA in the cytoplasm are thought to cause circularization of the message and increase the efficiency of translation (*3*). Polyadenylation of mRNA is also observed in prokaryotes and appears to facilitate mRNA degradation (*4*).

Poly(A) tails are formed by a multiprotein complex which recognizes a polyadenylation signal at the 3′ end of a nascent transcript and cleaves the precursor RNA. PAP then adds the poly(A) tail [reviewed in (*5*)]. PAPs are well conserved across phyla with the first ~400 amino acids showing considerable sequence identity (*6*). The catalytic function of PAP resides in its NH_2-terminal domain (*7*), which shows sequence similarity to members of the nucleotidyl transferase (NT) family that includes DNA polymerase β (Polβ), CCA-adding enzymes, and several bacterial antibiotic resistance enzymes (*8*). Pap1 retains polymerase activity when separated from the holoenzyme assembly and can processively add long stretches of adenosine nucleotides to an RNA primer in vitro. Although it employs the same catalytic mechanism as other nucleic acid polymerases, PAP is significantly different in that it does not utilize a template strand to select and position the incoming nucleotide.

We have determined the the structure of both the apo and 3′-dATP–bound states of a Pap1 truncation mutant (Δ10PAP), which contains the NH_2-terminal 537 of the 568 amino acids in wild-type Pap1 (*9*). This truncated enzyme exhibits wild-type activity in vitro and is capable of rescuing an otherwise lethal disruption of the yeast PAP1 gene (*10*). Crystals formed from Δ10PAP contain two copies of Pap1 in the asymmetric unit cell (ASU). The structure was first solved to 3.2 Å by selenomethionine multiwavelength anomalous diffraction (MAD), and later refined against higher resolution data sets with and without 3′-dATP and divalent cations soaked into the crystals (Table 1) (*11*).

At first glance, Pap1 looks like many other polymerases. A large 20 Å by 30 Å by 45 Å cleft is bounded by three globular domains (Fig. 1). In other polymerases, this arrangement has been likened to a hand in which the substrates are held between the thumb and fingers and presented to an active site in the palm (Fig. 1, inset) (*12*). Pap1 differs from these polymerases, however, in that the

[1]Boston Biomedical Research Institute, 64 Grove Street, Watertown, MA 02472, USA. [2]Tufts University School of Medicine, Department of Molecular Microbiology, Boston, MA 02111, USA. [3]Macromolecular Crystallography Facility at the Advanced Light Source (ALS), Physical Biosciences Division, Lawrence Berkeley National Laboratory, Berkeley, CA 94720, USA. [4]Tufts University School of Medicine, Department of Biochemistry, Boston, MA 02111, USA.

*To whom correspondence should be addressed. E-mail: bohm@bbri.org